Nonadiabatic effects in the dynamics of atoms confined in a cylindric time-orbiting-potential magnetic trap

Nonadiabatic effects in the dynamics of atoms confined in a cylindric time-orbiting-potential magnetic trap

Roberto Franzosi*
INFN Sez. di Pisa and INFM UdR di Pisa, Dipartimento di Fisica E. Fermi Università di Pisa, Via Buonarroti 2, I-56127 Pisa, Italy.

Andrea Spinelli, Bruno Zambon,† and Ennio Arimondo
INFM UdR di Pisa, Dipartimento di Fisica E. Fermi Università di Pisa, Via Buonarroti 2, I-56127 Pisa, Italy.

(Dated: November 1, 2018)

In a time-orbiting-potential magnetic trap the neutral atoms are confined by means of an inhomogeneous magnetic field superimposed to an uniform rotating one. We perform an analytic study of the atomic motion by taking into account the nonadiabatic effects arising from the spin dynamics about the local magnetic field. Geometric-like magnetic-fields determined by the Berry's phase appear within the quantum description. The application of a variational procedure on the original quantum equation leads to a set of dynamical evolution equations for the quantum average value of the position operator and of the spin variables. Within this approximation we derive the quantum-mechanical ground state configuration matching the classical adiabatic solution and perform some numerical simulations.

PACS numbers: 32.80.Pj, 03.65.Bz, 45.50.-j

I. INTRODUCTION

The difficulty of analysing a complex physical system is greatly reduced when one is able to identify a certain number of different time scales present in the system dynamical evolution. Thus, a series of approximations, generically termed adiabatic approximations, can successfully be carried out. The very simple basic idea is that of dealing first with the motion of the fast variables, keeping the slow ones fixed but arbitrary, and then to complete the analysis of the entire system by allowing a variation of the previously fixed coordinates. The quantum adiabatic theorem and the molecular Born-Oppenheimer approximation are well-known examples of this approach, with its origins in the early days of quantum mechanics. The quantum-adiabatic theorem dictates that a system prepared in an eigenstate of its Hamiltonian will remain in the corresponding eigenstate as the Hamiltonian is varied slowly enough. If the Hamiltonian returns to its original form, the system assumes the original eigenstate multiplied by an appropriate dynamical phase factor related to the instantaneous eigenvalue of the Hamiltonian. Berry made the interesting observation that in addition to the dynamical phase factor produced by the eigenvalue time evolution, the wavefunction acquires an additional phase contribution [1]. This additional contribution, the geometric phase, depends only on the path travelled by the system in the space of external parameters.

A canonical example for a system where this behavior occurs is that of a neutral particle carrying a magnetic moment and moving in an inhomogeneous magnetic field. Here, the fast variable is the transverse magnetic moment, and the slow variable is the atomic position and momentum [2]. If the magnetic field varies slowly enough in space, the effective Hamiltonian governing the dynamics of the slow external variables contains an induced gauge potential, the so-called geometric potential. In the classical limit the gauge geometric fields acting on the neutral particle with a magnetic moment have been studied by Aharonov and Stern [3]; they found that the atom experiences geometric Lorentz-type and electric-type forces [4]. The magnitudes of these forces do not depend on the amplitude of the magnetic field, but only on its local orientation.

In order to treat the non-adiabatic corrections improved Born-Oppenheimer methods were introduced for the case of arbitrary spin values [5]. Later the non-adiabatic terms modifying the atomic motion have been studied by several authors in the context of magnetic structures guiding or confining very cold atoms [6, 7, 8, 9]. The non-adiabatic corrections produce spin-flip transitions leading to atomic loss from the magnetic configurations, and also they modify the atomic motion. High order post-adiabatic corrections, leading to geometric electromagnetism potentials, have been investigated for the elegant configuration of an atom orbiting around a straight current-carrying wire [10]. For the verification of Berry's phase and its consequences a natural question is whether one can observe the direct modification of the atomic motion in the classical limit for the induced gauge potentials. Measurements on the motion of a rubidium Bose-Einstein condensate in a time-orbiting-potential (TOP) magnetic trap represent a quite strong indication for the existence of these geometric forces [11, 12]. Those observations were analyzed through a classical description for the condensate center-

*Electronic address: Roberto.Franzosi@df.unipi.it
†Electronic address: Bruno.Zambon@df.unipi.it

of-mass motion and for the atomic magnetic moment.

In the present paper we perform an analytic study of the atomic quantum dynamics within TOP magnetic traps. We take into account the non-adiabatic effects arising from the dynamics of the spin orientation around the local magnetic field. Within a pure quantum description, the geometric magnetic fields appear as a consequence of the presence of inhomogeneous magnetic fields. In this context spinors quantities can be introduced to describe the atomic spin states, as done by Ho and Shenoy [6] for the Berry phase in atomic condensates in magnetic traps. We derive an effective atomic dynamics, by means of a time-dependent variation principle making the quantum description analytically treatable. Thus, the atomic motion results by the coupling of a quantum harmonic motion, governing the atomic scalar wave function, and an effective nonlinear spin dynamics. The harmonic Hamiltonian depends on time-varying parameters that, in turns, are linked to the spin state. Also the spin Hamiltonian parameters are time-dependent, as they result from the atomic wave-functions expectation values of the above geometric operators. Within this non-adiabatic approximation the ground state configuration matches well the adiabatic solution. We also performed numerical simulations with these new equations. For the parameters suggested by the standard experimental set-up we found that the adiabatic approximation is well suited. Nevertheless, by reducing the intensity of the bias field, non-adiabatic effects show up, because under these conditions the influence of the geometric fields is more relevant.

Section II summarizes the classical analysis based on the adiabatic approximation and leading to the atomic micromotion. Section III reports a quantum analysis of the atomic motion within the adiabatic approximation by taking into account the lowest frequency terms of the time-dependent potential. Within this approximation we recover the quantum counterpart of the classical micromotion. Section IV studies the quantum dynamics of atoms into TOP traps. In Section V, by means of a time-dependent-variation-principle, we derive an effective dynamics for the atomic motion. Section VI reports numerical simulations for the dynamical regime of the atomic motion.

II. TOP TRAP

Bose-Einstein condensation in dilute atomic gas is created by trapping cold atoms in a magnetic trap of which the Ioffe-Pritchard (IP) and the time-orbiting-potential are the most common ones. In a TOP trap the magnetic field, schematically represented in the inset of Fig. 1, is composed of a quadrupole (inhomogeneous) field and a rotating (time-dependent) bias field, B_0. The TOP trap, introduced in [13] for the very first experiments on Bose-Einstein condensation [14], is employed by a number of research groups producing Bose-Einstein condensates [15, 16, 17, 18, 19].

The single particle Hamiltonian for the atoms inside a magnetic field configuration which characterizes the trap geometry is given by

$$H(t) = \frac{\mathbf{p}^2}{2m} + mgz - \frac{\mu}{s}\mathbf{s}\cdot\mathbf{B}(\mathbf{x},t) \tag{1}$$

where $\mathbf{s}$ are the spin operators of the $s = \hbar j$ representation, the last term takes into account the magnetic interaction energy of an atom with magnetic moment $\mu\mathbf{s}/s$ and projection $\mu = -|\mu|$ along the magnetic field $\mathbf{B}$. We also adopt the representation $\mathbf{x} = x\hat{x} + y\hat{y} + z\hat{z}$ for the position vector. For a TOP trap the magnetic field is the superposition of a static quadrupole field and one rotating at the radiofrequency (RF) ω_T

$$\mathbf{B}(\mathbf{x},t) = \mathbf{b}(\mathbf{x}) + \mathbf{B}_t(t)\,. \tag{2}$$

Its components are

$$\mathbf{b}(\mathbf{x}) = b_x x\hat{x} + b_y y\hat{y} + b_z z\hat{z}\,. \tag{3}$$

and

$$\mathbf{B}_t(t) = B_0\cos(\omega_T t)\hat{x} + B_0\sin(\omega_T t)\hat{y}\,. \tag{4}$$

The magnetic field parameters define the specific type of TOP trap we are analyzing [21]. By supposing the RF field rotating in the horizontal x, y plane we define the TOP geometry of the traps operating at Boulder [13] and at Pisa [22]. In this work we analyze the dynamics of a cylindric TOP trap with

$$b_x = b_y = -b_z/2 = b\,. \tag{5}$$

For the usual TOP trap three different time scales exists: the fastest motion, given by the Larmor frequency ω_L and related to the spin precession around the local magnetic field; the magnetic bias field rotating frequency ω_T giving rise to time-dependent forces at the frequences $\omega_T, 2\omega_T, \ldots$ and a slower motion associated to the atom spatial motion given by the trap harmonic frequency ω_h. These time scales are in order of magnitude, i.e. $\omega_h << \omega_T << \omega_L$ thus making possible the adiabatic approximation. In the first place the fast spin precession around the local magnetic field allows to consider the atoms spin locked to the local magnetic field throughout the whole spatial motion. This leads to an adiabatic time dependent potential $U = -\frac{\mu}{s}\mathbf{s}\cdot\mathbf{B}(\mathbf{x},t) = |\mu|\cdot|\mathbf{B}(\mathbf{x},t)|$. Secondly by averaging in time (over a period $2\pi/\omega_T$) this potential and by keeping only the slowest component gives rise to a harmonic potential spatially confining the condensate. The next order of approximation examines the fast variables (fast with respect to the harmonic dynamics at frequency ω_h) related to the time-dependent potential (at frequency ω_T). An exhaustive computation of this approximation is found in [23].

Gov *et al* [20] have used the standard classical equations of the atomic motion of a magnetic moment within a

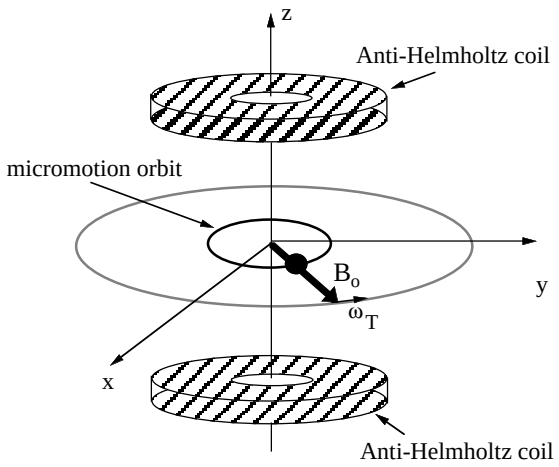

FIG. 1: Schematic representation of a cylindric TOP trap with the anti-Helmholtz coils producing a quadrupole field with vertical symmetry, the B_0 bias field rotating at angular frequency $\omega_{\rm T}$ in the horizontal plane, and the atomic cloud (black sphere) following the micromotion orbit.

TOP in which all the different time scales are present. In this context a steady periodic orbit can be found exactly without resorting to any approximation. This periodic solution corresponds to what it is known as the *atomic micromotion* [24] (see Fig. 1). As the atoms trace out the atomic micromotion orbit, the magnitude and direction of the local magnetic field change in space and time, with the magnetic moment of the atom precessing around the direction of the field. In fact, given the Hamiltonian of Eq. (1) a dynamical state $|\Psi\rangle$ satisfies the following center-of-mass equations of motion:

$$\begin{aligned} m\frac{d^2\mathbf{R}}{dt^2} &= \frac{\mu}{s}\nabla[\mathbf{S}\cdot\mathbf{b}(\mathbf{R})] - mg\hat{z} \\ \frac{d\mathbf{S}}{dt} &= \frac{\mu}{s}\langle\Psi|\mathbf{s}\wedge\mathbf{B}(\mathbf{x},t)|\Psi\rangle\,, \end{aligned} \tag{6}$$

where $\mathbf{R} = X\hat{x} + Y\hat{y} + Z\hat{z} = \langle\Psi|\mathbf{x}|\Psi\rangle$ is the expectation value of the center of mass position, and $\mathbf{S} = S_x\hat{x} + S_y\hat{y} + S_z\hat{z} = \langle\Psi|\mathbf{s}|\Psi\rangle$ is the expectation value of the atomic spin.

Thus we are lead to a set of equations which are not closed. However if the quantum mechanical wave function can be factorized, as to the lowest order approximation, we may write $\langle\mathbf{s}\wedge\mathbf{B}(\mathbf{x},t)\rangle = \langle\mathbf{s}\rangle\wedge\langle\mathbf{B}(\mathbf{x},t)\rangle$. Within this approximation the above system of equations becomes closed and assumes the form

$$\begin{aligned} m\frac{d^2\mathbf{R}}{dt^2} &= \frac{\mu}{s}\nabla[\mathbf{S}\cdot\mathbf{b}(\mathbf{R})] - mg\hat{z} \\ \frac{d\mathbf{S}}{dt} &= \frac{\mu}{s}\mathbf{S}\wedge\mathbf{B}(\mathbf{R},t)\,. \end{aligned} \tag{7}$$

The simplest periodic solutions generated by the Eqs. (7) give a good estimate of the fast center-of-mass condensate dynamics, i.e. the atomic micromotion. This motion was experimentally observed in a triaxial TOP trap in Ref. [11]. This periodic solution is best viewed in a frame rotating with the bias magnetic field. In this frame the magnetic moment results to be aligned to the effective magnetic field and the atomic center of mass is at rest. Also, in order to have a stable motion, the spin must be tuned to the effective magnetic field, producing a confining potential energy. The stability along the z axis requires a zero force along this direction: this leads to

$$\frac{S_z}{s} = \frac{m\,g}{2b|\mu|} = \xi \tag{8}$$

which accounts for the fact that the component of the spin along z must be positive. The centrifugal force balancing the gradient force yields the radius of the micromotion

$$r = \frac{|\mu|b}{m\omega_T^2}\alpha \qquad \alpha = \sqrt{1-\xi^2} \tag{9}$$

where ξ and α are respectively the cosinus and sinus that the effective field $\mathbf{B}^{inst}$ forms with the z axis. The components of the effective field in the rotating frame, with horizontal component along the x axis, are

$$B_x^{inst} = b\,r \qquad \text{and} \qquad B_z^{inst} = -2\,b\,z + \omega_T s/\mu. \tag{10}$$

In order to determine the z height of the periodic orbit under examination, the following parameters also useful in the subsequent analysis are required:

$$\varsigma = \frac{\omega_T s}{\mu b}, \quad \rho = \frac{B_0}{b}\,. \tag{11}$$

ρ being the radius of the circle of death [13] and ς is twice the amount the zero point of the quadrupole field shifts downwards for effect of the uniform fictitious magnetic field which appears in the rotating frame. In terms of these parameters the equilibrium height can be expressed by means of the following alignment relation

$$\frac{-2\,b\,(z-\frac{\varsigma}{2})}{B_0 + b\,r} = \frac{\xi}{\sqrt{1-\xi^2}} \tag{12}$$

which leads to

$$z = \frac{\varsigma}{2} - \frac{\xi}{\sqrt{1-\xi^2}}\left(\frac{B_0 + b\,r}{2b}\right) = \frac{\varsigma}{2} - \frac{\xi}{2}\left(\frac{\rho}{\alpha} + \frac{|\mu|b}{m\,\omega_T^2}\right) \tag{13}$$

The above analysis suggest that the adiabatic approximation is more rigorous if we refer to $\mathbf{B}^{inst}$ instead of the real magnetic field. Indeed, in the motion described above the adiabatic approximation is completely fulfilled with respect to this field. However, for more general solutions of the Eqs. (7) the behavior is different and we must also account for a spin component orthogonal to the local magnetic field. In any case, as it will be shown in the numerical simulations, the projection of the magnetic moment along this field is a much better conserved

quantity with respect to that along the real field. In Refs. [3, 25] the effect of the components perpendicular to the real magnetic field have been examined and it was found that a small misalignment with respect to this field gives rise to a Lorentz-type force. An additional electric-type force is originated by the time average of the fast oscillatory force induced by the spin precession. Both kind of forces, affecting the center-of mass dynamics, are geometric forces because they do not depend on the magnitude of the magnetic field but only on its orientation.

III. FROM CLASSICAL TO QUANTUM ADIABATIC APPROXIMATION

The gross features of the atomic confinement in a magnetic trap are explained in terms of the adiabatic approximation. If this is fulfilled, an atom with electron magnetic moment parallel to the local magnetic field experiences a confining potential given by $U = |\mu \mathbf{B}|$. Working in the rotating frame one replaces $\mathbf{B}$ with $\mathbf{B}^{inst}$. Since in the following we will make use of an adiabatic-like solution in order to find non-adiabatic corrections, we will assume the spin to form an angle with $\mathbf{B}^{inst}$, whence we will take the spin component in the direction of the instantaneous magnetic field to be $s\sigma = \mathbf{s}\cdot\mathbf{B}^{inst}/|\mathbf{B}^{inst}|$. Thus, from Eq. (1) we obtain the adiabatic Hamiltonian to be

$$H^{\sigma}_{ad} = \frac{\mathbf{p}^2}{2m} + U_{ad}\,, \tag{14}$$

where

$$\begin{aligned} U_{ad} = mgz + \sigma|\mu|\Big[(bx + B_0\cos\omega_T t)^2 + \\ (by + B_0\sin\omega_T t)^2 + (-2bz + \frac{\omega_T s}{\mu})^2\Big]^{1/2}\,. \end{aligned} \tag{15}$$

For small displacements of the atoms from the equilibrium position $(0,0,h)$, the adiabatic potential U_{ad} can be expanded in a power series of the displacement coordinates $(x, y, \zeta = z - h)$, and up to the second order we have

$$\begin{aligned} U^{(2)}_{ad} = &+ mg\left(1 + \frac{\sigma\eta}{\beta\xi}\right)\zeta + \\ &\frac{1}{2}m\left[\omega^2_{0,r}(x^2+y^2) + \omega^2_{0,z}\zeta^2\right] + U_0 + U(t)\,. \end{aligned} \tag{16}$$

Here the time-independent component is

$$U_0 = mgh + \sigma\beta|\mu|B_0\,, \tag{17}$$

and the time-dependent component is

$$\begin{aligned} U(t,\sigma) = \frac{\sigma|\mu|b}{\beta}\left(1 - \frac{2\eta}{\beta^2}\frac{\zeta}{\rho}\right)(x\cos\omega_T t + y\sin\omega_T t) - \\ \frac{\sigma|\mu|b}{4\rho\beta^3}\left[(x^2-y^2)\cos(2\omega_T t) + 2xy\sin(2\omega_T t)\right]\,. \end{aligned} \tag{18}$$

The new adimensional constants here introduced are

$$\eta = \frac{2h - \varsigma}{\rho}\,, \quad \beta = \sqrt{1+\eta^2}\,,$$

while the oscillation frequencies are

$$\omega_{0,r} = \sqrt{\frac{\sigma|\mu|b(2\eta^2+1)}{2m\rho\beta^3}}\,, \quad \omega_{0,z} = \sqrt{\frac{4\sigma|\mu|b}{m\rho\beta^3}}\,. \tag{19}$$

Two time scales are involved in $U^{(2)}_{ad}$, the slower one being associated to the harmonic motion at the oscillation frequencies $\omega_{0,r}$ and $\omega_{0,z}$, whereas the faster one is associated with the bias frequency ω_T. The oscillating forces have vanishing time average over a period $2\pi/\omega_T$. This can be substantiated by the following wave function factorization

$$\Psi(\mathbf{x}, t, \sigma) = \Phi(\mathbf{x}, t, \sigma)\mathcal{E}(\mathbf{x}, t, \sigma) \tag{20}$$

where

$$\mathcal{E} = \exp[-iw/\hbar], \tag{21}$$

and $w = \int_0^t dt U(t,\sigma)$ describes the dominant effects of the oscillating potential. The time-scale separation allows us to consider $\Phi(\mathbf{x}, t)$ as a slowly varying function of time [26]. Notice the explicit dependence on the parameter σ. Substituting Eq. (20) into the Schrödinger equation with the potential $U^{(2)}_{ad}$, we get

$$\begin{aligned} i\hbar\partial_t\Phi(\mathbf{x},t,\sigma) = &\left[\frac{\mathbf{p}^2}{2m} + U_0 + (mg + \frac{\sigma\eta}{\beta\xi})\zeta + \right. \\ &\left.\frac{1}{2}m\left[\omega^2_{0,r}(x^2+y^2) + \omega^2_{0,z}\zeta^2\right]\right]\Phi(\mathbf{x},t,\sigma) + \\ &\left[\frac{i\hbar}{m}\nabla w\cdot\nabla + \frac{1}{2m}|\nabla w|^2 + \frac{i\hbar}{2m}\nabla^2 w\right]\Phi(\mathbf{x},t,\sigma)\,, \end{aligned} \tag{22}$$

The above assumptions on the different timescales allow us to consider the coefficients of the oscillating terms at frequencies ω_T and $2\omega_T$ as slowly varying ones. Indeed a time average over the short time $2\pi/\omega_T$ leads to

$$\begin{aligned} i\hbar\partial_t\Phi(\mathbf{x},t,\sigma) = &\left\{\frac{\mathbf{p}^2}{2m} + mg\left(1 + \frac{\sigma\eta}{\beta\xi} - \frac{\sigma^2\eta}{2\rho\beta^4\xi^2}\frac{g}{\omega^2_T}\right)\zeta + \right. \\ &\left.\frac{1}{2}m\left[\omega^2_r(x^2+y^2) + \omega^2_z\zeta^2\right]\right\}\Phi(\mathbf{x},t)\,, \end{aligned} \tag{23}$$

where the irrelevant constant terms have been dropped. This equation displays a three-dimensional harmonic oscillator structure whose frequences are

$$\begin{aligned} \omega_r &= \omega_{0,r}\left[1 + \frac{\sigma}{16\xi\beta^3}\frac{g}{\rho\omega^2_T}\frac{(32\eta^2+1)}{(2\eta^2+1)}\right]^{1/2}\,, \\ \omega_z &= \omega_{0,z}\left[1 + \frac{\sigma}{2\beta^3}\frac{g}{\rho\omega^2_T}\eta^2\right]^{1/2} \end{aligned} \tag{24}$$

in the xy-plane and along the z-direction, respectively. The equilibrium position along the z-axis is obtained by setting to zero the term multiplying ζ in Eq. (23). Neglecting smaller contributions, the equilibrium atomic position is given by

$$h(\sigma) = \varsigma/2 - \rho\xi/(2\sqrt{\sigma^2 - \xi^2})\,. \tag{25}$$

In the limit $\sigma = 1$ the classical solution of Eq. (13) up to a small term containing ω_T^{-2} is matched. The expectation value of the particle momentum $\mathbf{p}$ on the state (20) is

$$\langle \mathbf{p} \rangle = \frac{|\mu| b \sqrt{\sigma^2 - \xi^2}}{\omega_T} (-\sin\omega_T t, \cos\omega_T t, 0)\,. \tag{26}$$

This result is only in part equivalent to the classical one of Eq. (13) because here the instantaneous position value $\langle \mathbf{x} \rangle$ is always zero.

IV. QUANTUM DYNAMICS

A. Effective Hamiltonian

The quantum dynamics is more properly addressed by transforming the original equations into a spin reference frame rotating at the bias field frequency. Thus the wave function $|\Psi^{\mathrm{R}}\rangle$ in the rotating frame is written as $|\Psi^{\mathrm{R}}\rangle = R_z(-\omega_T t)|\Psi\rangle = exp(\frac{i}{\hbar} s_z \omega_T t)|\Psi\rangle$, where $R_z(\vartheta)$ is the rotation around the z axis by an angle ϑ, and $|\Psi\rangle$ is the laboratory frame wave function. Then the Schrödinger equation for $|\Psi^{\mathrm{R}}\rangle$ becomes

$$\begin{aligned} i\hbar\partial_t|\Psi^{\mathrm{R}}\rangle =& i\hbar\partial_t R_z(-\omega_T t)|\Psi\rangle = \\ & [H'(t) - \hbar\omega_T s_z]|\Psi^{\mathrm{R}}\rangle \;= H^{\mathrm{R}}|\Psi^{\mathrm{R}}\rangle, \end{aligned} \tag{27}$$

where $H'(t) = R_z(-\omega_T t) H(t) R_z(\omega_T t)$ is time-dependent and

$$H^{\mathrm{R}} = H'(t) - \hbar\omega_T s_z = \frac{\mathbf{p}^2}{2m} + mgz - \frac{\mu}{s}\mathbf{s}\cdot\mathbf{B}^{\mathrm{R}}(\mathbf{x}, t)\,, \tag{28}$$

with $\mathbf{B}^{\mathrm{R}}(\mathbf{x}, t) = [B_0 + b(x\cos\omega_T t + y\sin\omega_T t)]\hat{x} + b(y\cos\omega_T t - x\sin\omega_T t)\hat{y} + (-2bz + \omega_T s/\mu)\hat{z}$. $\mathbf{B}^{\mathrm{R}}$ is the magnetic field in the spin rotating frame, a constant bias field and a rotating inhomogeneous field. This effective magnetic field $\mathbf{B}^{\mathrm{R}}(\mathbf{x}, t) = B_x^{\mathrm{R}}\hat{x} + B_y^{\mathrm{R}}\hat{y} + B_z^{\mathrm{R}}\hat{z}$ identifies the position dependent angles ϑ and φ as

$$\vartheta = \arctan\frac{\sqrt{(B_x^{\mathrm{R}})^2 + (B_y^{\mathrm{R}})^2}}{B_z^{\mathrm{R}}}\,, \quad \varphi = \arctan\frac{B_y^{\mathrm{R}}}{B_x^{\mathrm{R}}}\,. \tag{29}$$

and $B^{\mathrm{R}} = \sqrt{(B_x^{\mathrm{R}})^2 + (B_y^{\mathrm{R}})^2 + (B_z^{\mathrm{R}})^2}$.

B. Local basis

It is useful to introduce a coordinate-dependent spin basis $\{|\chi_m(\mathbf{x}, t)\rangle\}$ such that

$$\frac{\mathbf{s}\cdot\mathbf{B}^{\mathrm{R}}(\mathbf{x}, t)}{B^{\mathrm{R}}}|\chi_m(\mathbf{x}, t)\rangle = m|\chi_m(\mathbf{x}, t)\rangle \quad \text{for } -j \le m \le j\ . \tag{30}$$

The local basis vectors in which the $z-$axis coincides with the magnetic field in the same point can be given in terms of the angles ϑ and φ through the rotation operator $M(\varphi, \vartheta)$ as follows

$$|\chi_m(\vartheta, \varphi)\rangle = M(\varphi, \vartheta)|j, k\rangle = e^{-\frac{i}{\hbar}\varphi s_z} e^{-\frac{i}{\hbar}\vartheta s_y}|j, k\rangle\,. \tag{31}$$

With the total wave function expanded as $|\Psi^{\mathrm{R}}\rangle = \sum_{m=-j}^{j} \psi^m(\mathbf{x}, t)\,|\chi_m(\mathbf{x}, t)\rangle$, the Hamiltonian of Eq. (28) becomes

$$\begin{aligned} H^{\mathrm{R}} =& \frac{\mathbf{p}^2}{2m} + mgz - \frac{\mu}{s}B^{\mathrm{R}}(\mathbf{x})s_z + \\ & \frac{1}{2m}\left\{2\mathbf{A}\cdot\mathbf{p} + \mathbf{p}(\mathbf{A}) + \mathbf{A}^2\right\} + \mathcal{V} \end{aligned} \tag{32}$$

with

$$\begin{aligned} \mathbf{A} &= -(s_z\cos\vartheta - s_x\sin\vartheta)\nabla\varphi - s_y\nabla\vartheta\,, \\ \mathcal{V} &= -(s_z\cos\vartheta - s_x\sin\vartheta)\partial_t\varphi - s_y\partial_t\vartheta\,. \end{aligned} \tag{33}$$

Appendix A contains details useful to derive the functions in Eq. (33). In Eq. (32) $\mathbf{A}$ and $\mathcal{V}$ represent pseudopotentials connected to the Lorentz-like and electric-like kinds of forces introduced in Ref. [3]. The functions $\varphi(\mathbf{x}, t)$ and $\vartheta(\mathbf{x}, t)$ depend on the effective magnetic field geometry as stated in Eqs. (29). Berry's geometric terms appear in the quantum Hamiltonian through these angles. By direct computation the following relations are derived:

$$\begin{aligned} \nabla\vartheta &= \frac{\left[\mathbf{B}^{\mathrm{R}} \wedge (\mathbf{B}^{\mathrm{R}} \wedge \nabla\mathbf{B}^{\mathrm{R}})\right]_z}{(B^{\mathrm{R}})^2\sqrt{(B^{\mathrm{R}})^2 - (B_z^{\mathrm{R}})^2}}\,, \quad \nabla\varphi = \frac{\left[\mathbf{B}^{\mathrm{R}} \wedge \nabla\mathbf{B}^{\mathrm{R}}\right]_z}{(B^{\mathrm{R}})^2 - (B_z^{\mathrm{R}})^2}\,, \\ \partial_t\vartheta &= \frac{\left[\mathbf{B}^{\mathrm{R}} \wedge (\mathbf{B}^{\mathrm{R}} \wedge \partial_t\mathbf{B}^{\mathrm{R}})\right]_z}{(B^{\mathrm{R}})^2\sqrt{(B^{\mathrm{R}})^2 - (B_z^{\mathrm{R}})^2}}\,, \quad \partial_t\varphi = \frac{\left[\mathbf{B}^{\mathrm{R}} \wedge \partial_t\mathbf{B}^{\mathrm{R}}\right]_z}{(B^{\mathrm{R}})^2 - (B_z^{\mathrm{R}})^2}\,. \end{aligned} \tag{34}$$

These terms, invariant with the modulus of the magnetic field, are geometric fields depending only on the force lines of the magnetic field, i.e., the field geometry. Their explicit form is given in Appendix B.

Notice that, starting from the Hamiltonian (1), which is linear in the spin operators, the nonadiabatic terms give rise to a dynamics with a quadratic dependence in the spins. We may write H^{R} in a form that put this in more evidence

$$H^{\mathrm{R}} = \frac{\mathbf{p}^2}{2m} + mgz + \sum_i h^i s_i + \sum_{jk} g^{jk} s_j s_k\,, \tag{35}$$

where the indices (i,j,k) run on (x,y,z), and the spin coefficients are

$$\begin{aligned}
h^x &= \frac{1}{2m}[\mathbf{p}\sin\vartheta\nabla\varphi + \sin\vartheta\nabla\varphi\mathbf{p}] + \sin\vartheta\partial_t\varphi\,,\\
h^y &= -\frac{1}{2m}[\mathbf{p}\nabla\vartheta + \nabla\vartheta\mathbf{p}] - \partial_t\vartheta\,,\\
h^z &= -\frac{\mu}{s}B^{\mathrm{R}} - \frac{1}{2m}[\mathbf{p}\cos\vartheta\nabla\varphi + \cos\vartheta\nabla\varphi\mathbf{p}] - \cos\vartheta\partial_t\varphi\,,\\
g^{xx} &= \frac{1}{2m}\sin^2\vartheta|\nabla\varphi|^2\,,\\
g^{yy} &= \frac{1}{2m}|\nabla\vartheta|^2\,,\\
g^{zz} &= \frac{1}{2m}\cos^2\vartheta|\nabla\varphi|^2\,,\\
g^{xz} &= g^{zx} = -\frac{1}{2m}\sin\vartheta\cos\vartheta|\nabla\varphi|^2\,.
\end{aligned} \tag{36}$$

and $g^{jk}=0$ otherwise. Let us recall that all the operators h_i, g_{jk} are hermitian ones.

V. BEYOND THE ADIABATIC APPROXIMATION

A. Effective spin dynamics

Since the exact solution of the Schrödinger Eq. (27) is an impracticable task, the spin dynamics will be taken into account in an effective way by resorting to a time-dependent variational principle (TDVP) [27]. The TDVP procedure allows to reduce the system quantum dynamics to a semiclassical Hamiltonian form. This procedure was introduced for studying the low-lying collective states in nuclei [28], but was later shown to provide a valid approximation also for the one particle Schrödinger equation. Within this procedure, whose details are shown in Appendix C, we choose a suitable trial state of the form

$$\psi(\mathbf{x},t) = \exp[-i\mathcal{S}(t)/\hbar]\Psi(\mathbf{x},t)|j,\tau(t)\rangle \tag{37}$$

which will be subjected to the weaker form of the Schrödinger equation embodied into TDVP, i.e. Eq. (C1) in Appendix C. Here $\Psi(\mathbf{x},t)$ and $|j,\tau(t)\rangle$ take in account for the center-of-mass motion and spin dynamics, respectively. $\mathcal{S}(t)$ is an effective action for the spin variables. By carrying out the variational procedure on the trial wave function we derive the classical equations of motion for the expectation-values of the spin-operators s_j on the spin component of the dynamical trial state $|j,\tau(t)\rangle$. A key point in this variational procedure is the parametrization of the spin variables in terms of coherent atomic states. These latter have the physical significance of angular momentum states produced by a classical source [28]. They depend on a complex parameter τ and are defined as

$$|j,\tau\rangle = \frac{1}{[1+|\tau|^2]^j}\sum_{m=-j}^{j}\left[\binom{2j}{(j+m)}\right]^{1/2}\tau^{j+m}|j,m\rangle\,, \tag{38}$$

where $|j,n\rangle$ are the spin basis with the quantization axis taken along the direction of the local field. These states, analogous to the coherent states of the electromagnetic field, are defined within a subspace determined by the angular momentum j. Within this sub-space each state, completely defined by the complex number τ, is mapped onto the direction of a vector on a sphere by a projective transformation [27]. In our case this vector identifies the orientation of a classical spin with respect to a local frame having the z axis along the local magnetic field $\mathbf{B}^{\mathrm{R}}(\mathbf{x},t)$. This property can be understood by computing the expectation values of the spin components on $|j,\tau\rangle$. By keeping in mind the parametrization $\tau = -e^{-i\varphi'}\tan(\vartheta'/2)$ we find

$$\begin{aligned}
\mathcal{S}_{\mathrm{x}} &= \langle j,\tau|s_x|j,\tau\rangle = j\hbar\sin\vartheta'\cos\varphi'\,,\\
\mathcal{S}_{\mathrm{y}} &= \langle j,\tau|s_y|j,\tau\rangle = j\hbar\sin\vartheta'\sin\varphi'\,,\\
\mathcal{S}_{\mathrm{z}} &= \langle j,\tau|s_z|j,\tau\rangle = j\hbar\cos\vartheta'\,.
\end{aligned} \tag{39}$$

where ϑ' and φ' are the angles between the classical spin and the local magnetic field. The detail of the spin dynamics derivation are contained in the Appendix C. Their ruling equations are generated by the classical Hamiltonian of Eq. (C4).

Let us focus on the center-of-mass motion described by the wave function $\Psi(\mathbf{x},t)$ as in Eq. (20). The trapping potential obtained by the application of TDVP procedure as from Eq. (C2) can be expanded in a power series of the displacement coordinates around the trap center by keeping only the harmonic terms. As a matter of fact these terms depend on the quantity $\sigma(t)$, with $\sigma(t)$ given by

$$\sigma(t) = \frac{\mathcal{S}_z}{s}\,. \tag{40}$$

that coincide with the definition introduced previously within the adiabatic approximation. Since the evolution of this quantity is much slower than the bias-frequency ω_T ($\omega_z \ll \omega_T$), its time dependence is maintained in the ruling equations even after averaging over the short time scale of the bias field time dependent terms as done in order to arrive to Eq. (23). As a consequence the wave function solution of (23) can be written as

$$\Phi(\mathbf{x},t,\sigma) = \sum_{\{\mathbf{n}\}} c_{\mathbf{n}}\mathcal{E}_{\mathbf{n}}(t)\Phi_{\mathbf{n}}(\mathbf{x},\sigma)\,, \tag{41}$$

where the vector index means $\mathbf{n}=(n_1,n_2,n_3)$ along the three orthogonal directions, and the constants $c_{\mathbf{n}}$ are determined by the atomic initial conditions. The functions $\Phi_{\mathbf{n}}(\mathbf{x},\sigma)$ are the eigenfunctions of the three-dimensional

harmonic oscillator with eigenvalues

$$E_{\mathbf{n}}(\sigma) = U_0 + \frac{1}{2m}\left(\frac{\sigma\mu b}{\beta\omega_T}\right)^2 + \hbar\omega_r(\sigma)(n_1+n_2+1) + \hbar\omega_z(\sigma)(n_3+\frac{1}{2}), \tag{42}$$

and $\mathcal{E}_{\mathbf{n}}(t) = \exp[i\gamma_{\mathbf{n}}(t)/\hbar - i\int_0^t dt E_{\mathbf{n}}(\sigma(t))/\hbar]$ embodies also a geometric phase

$$\gamma_{\mathbf{n}}(t) = i\hbar\int_{\sigma(0)}^{\sigma(t)} d\sigma\left[\int d\mathbf{x}\bar{\Phi}_{\mathbf{n}}(\mathbf{x},\sigma)\frac{\partial}{\partial\sigma}\Phi_{\mathbf{n}}(\mathbf{x},\sigma)\right]. \tag{43}$$

The parameter $\sigma(t)$ entering into the equations of motion for the atomic center of mass is actually a dynamical degree of freedom whose evolution is generated by the classical spin dynamics. Thus, the center of mass motion and the spin dynamics interact the one with the other and they must be simultaneously integrated. Let us stress that the dynamics we have just found, is the classical canonical counterpart of that one generated by the full quantum Hamiltonian written in Eq. (35).

B. Ground state configuration

In order to find the non-adiabatic corrections to the ground state solution (20), we assume that this solution is well represented also if we keep the lowest order in the expression of the Hamiltonian of Eq. (C4), i.e., the first order in (x, y, ζ) appearing in H^R. This means that the Hamiltonian parameters of Eq. (C4), the classical form of Eq. (35), can be computed as an average on the adiabatic-like ground state solution of Eq. (20) of the approximated operators h^i, g^{jk}. Therefore at the lowest order of approximation the terms in Eq. (36) result

$$\begin{aligned}
h^x &\simeq \frac{1}{m\rho\beta}[-\sin(\omega_T t)p_x + \cos(\omega_T t)p_y],\\
h^y &\simeq -\frac{1}{m\rho\beta^2}\{\eta[\cos(\omega_T t)p_x + \sin(\omega_T t)p_y] + 2p_z\},\\
h^z &\simeq -\frac{\mu b\rho}{s}\beta - \frac{\eta}{m\rho\beta}[-\sin(\omega_T t)p_x + \cos(\omega_T t)p_y],\\
g^{xx} &\simeq \frac{1}{2m\rho^2\beta^2},\\
g^{yy} &\simeq \frac{3+\beta^2}{2m\rho^2\beta^4},\\
g^{zz} &\simeq \frac{\eta^2}{2m\rho^2\beta^2},\\
g^{xz} &\simeq -\frac{\eta}{2m\rho^2\beta^2}.
\end{aligned}$$

Recalling the expectation value of the momentum $\mathbf{p}$ given by Eq. (26), up to the order $1/\rho$ we have

$$\begin{aligned}
\langle h^x_{(0)}\rangle &\simeq \frac{2\beta}{(1+\eta^2)}\frac{\omega^2_{0,r}}{\omega_T},\\
\langle h^z_{(0)}\rangle &\simeq -\beta\frac{\mu B_0}{s} - \frac{2\eta\beta}{(1+\eta^2)}\frac{\omega^2_{0,r}}{\omega_T},
\end{aligned}$$

and 0 otherwise. The corresponding classical spin Hamiltonian is, apart a constant,

$$\mathcal{H}(\mathcal{S}_x,\mathcal{S}_y,\mathcal{S}_z) = \langle h^x_{(0)}\rangle\mathcal{S}_x + \langle h^z_{(0)}\rangle\mathcal{S}_z,$$

whose equations of motion results

$$\begin{aligned}
\dot{\mathcal{S}}_x &= -\langle h^z_{(0)}\rangle\mathcal{S}_y,\\
\dot{\mathcal{S}}_y &= -\langle h^x_{(0)}\rangle\mathcal{S}_z + \langle h^z_{(0)}\rangle\mathcal{S}_x,\\
\dot{\mathcal{S}}_z &= \langle h^x_{(0)}\rangle\mathcal{S}_y.
\end{aligned} \tag{44}$$

By setting $\dot{\mathcal{S}}_i = 0$ with $(i = x, y, z)$ we determine the ground state configuration

$$\begin{aligned}
(\mathcal{S}^0_x,\mathcal{S}^0_y,\mathcal{S}^0_z) = (&\pm\frac{\langle h^x_{(0)}\rangle}{\langle h^z_{(0)}\rangle}\frac{\hbar j}{\sqrt{1+\langle h^x_{(0)}\rangle^2/\langle h^z_{(0)}\rangle^2}}, 0,\\
&\pm\frac{\hbar j}{\sqrt{1+\langle h^x_{(0)}\rangle^2/\langle h^z_{(0)}\rangle^2}}).
\end{aligned} \tag{45}$$

The $\mathbf{S}^0$ solution, with the spin aligned to the local magnetic field, provides a correction to the adiabatic approximation discussed before.

C. Effective classical dynamics

The center of mass motion is described by the wavefunction $\Psi(\mathbf{x},t) = \Phi(\mathbf{x},t,\sigma)\mathcal{E}(\mathbf{x},t,\sigma)$ introduced in (37). The exponential factor $\mathcal{E}(\mathbf{x},t,\sigma)$ has been defined in Eq. (21) and $\Phi(\mathbf{x},t,\sigma)$ satisfies the time-dependent Schrödinger equation (23) for the 3-dimensional harmonic oscillator which Hamiltonian is $H = \mathbf{p}^2/(2m) + U_h(\mathbf{x},\sigma(t))$. In terms of the frequencies (24) and of the equilibrium atomic position (25), the time-dependent harmonic potential has the form $U_h(\mathbf{x},\sigma(t)) = m[\omega_r^2(\sigma(t))(x^2+y^2) + \omega_z^2(\sigma(t))(z-h(\sigma(t)))^2]/2$.

Upon introducing the center of mass position $\mathbf{R} = \langle\Psi|\mathbf{x}|\Psi\rangle$ and momentum $\mathbf{P} = \langle\Psi|\mathbf{p}|\Psi\rangle$, the following classical equations of motion are easily derived

$$\begin{aligned}
\frac{d\mathbf{R}}{dt} &= \frac{\mathbf{P}}{m},\\
\frac{d\mathbf{P}}{dt} &= -\nabla_{\mathbf{R}}U_h(\mathbf{R},\sigma(t)) - \frac{d\mathbf{\Delta P}}{dt}
\end{aligned} \tag{46}$$

where $\mathbf{\Delta P} = \int d\mathbf{x}|\Phi(\mathbf{x},t)|^2\nabla w(\mathbf{x},t)$, and $\sigma(t)$ is defined by Eq. (40). Now we introduce a further factorization of the kind $\langle\Psi|\mathcal{O}(\mathbf{x},t)\mathbf{p}|\Psi\rangle \approx \mathcal{O}(\mathbf{R},t)\mathbf{P}$, where $\mathcal{O}(\mathbf{x},t)\mathbf{p}$ stands for the first three among the operators appearing into Eqs. (36) expanded in a power series of $\mathbf{x}$ and $\mathbf{p}$ up to the second order [29]. Then by considering only the linear terms in spin variables appearing into the classical spin Hamiltonian (C4) we can write

$$\mathcal{H}(\mathcal{S}_{\rm x},\mathcal{S}_{\rm y},\mathcal{S}_{\rm z}) = \sum_i\langle h^i\rangle\mathcal{S}_i, \tag{47}$$

where the time-dependent coefficients are implicit in the center of mass wave function $\Psi(\mathbf{x},t)$ as given in (C5). Thus in Appendix C we derive the following equation of motion for the classical spin

$$\frac{d\mathcal{S}}{dt} = \mathcal{B}(t) \wedge \mathcal{S}\,. \tag{48}$$

where the magnetic field $\mathcal{B}$ is the sum of the real one plus some fictitious terms having originated from the geometric forces with components

$$\begin{aligned}
\mathcal{B}_x(t) &= \frac{\left\{\mathbf{B}^{\mathrm{R}} \wedge \left[\left(\frac{\mathbf{P}}{m}\cdot\nabla + \partial_t\right)\mathbf{B}^{\mathrm{R}}\right]\right\}_z}{B^{\mathrm{R}}\sqrt{(B_x^{\mathrm{R}})^2 + (B_y^{\mathrm{R}})^2}}\,,\\
\mathcal{B}_y(t) &= -\frac{\left\{\mathbf{B}^{\mathrm{R}} \wedge \left[\mathbf{B}^{\mathrm{R}} \wedge \left[\left(\frac{\mathbf{P}}{m}\cdot\nabla + \partial_t\right)\mathbf{B}^{\mathrm{R}}\right]\right]\right\}_z}{(B^{\mathrm{R}})^2\sqrt{(B_x^{\mathrm{R}})^2 + (B_y^{\mathrm{R}})^2}}\,,\\
\mathcal{B}_z(t) &= -\frac{\mu}{s}B^{\mathrm{R}} - \frac{B_z^{\mathrm{R}}\left\{\mathbf{B}^{\mathrm{R}} \wedge \left[\left(\frac{\mathbf{P}}{m}\cdot\nabla + \partial_t\right)\mathbf{B}^{\mathrm{R}}\right]\right\}_z}{B^{\mathrm{R}}[(B_x^{\mathrm{R}})^2 + (B_y^{\mathrm{R}})^2]}\,.
\end{aligned} \tag{49}$$

Thus, the two equations systems (46) and (48) form a closed system to be simultaneously integrated.

VI. NUMERICAL SIMULATIONS

We have numerically integrated the set of equations (46) and (48) by means of a Runge-Kutta algorithm. The set of parameters chosen, i.e. $B_0 = 4.\ 10^{-4}$T, $b = 0.18$T/m, and $\omega_T = 2\pi\ 10^4\mathrm{s}^{-1}$, correspond to those used in TOP experiments exploring the rubidium micromotion [11, 12]. The simulations allowed to recover the atomic micromotion, representing periodic closed orbits. The micromotion was investigated through the classical equations of motion (7) and also through the improved system of equations of Eqs. (46) and (48). Similar results were obtained for the center of mass motion. In both approaches we observed a strong dependence on the initial conditions, that for the classical center of mass variables are given by Eqs. (25) and (26). For the spin variable the classical condition corresponds to the spin aligned along the local $\mathbf{B}^{inst}$ magnetic field, while the quantum mechanical solution requires the atom to be in an eigenstate of the spin operator along the local magnetic field. A modification of the initial conditions from those required for the atomic micromotion, for instance a shift of 100 μm along the $z-$axis, produced the open trajectories shown in Fig. 2. We noticed also a strong dependence on the initial condition for the atomic spin. We also verified that within the parameters used here which approximately match those corresponding to the experimental set up of Ref. [11], the correction to the adiabatic approximation expressed by Eq. (45) are not quite relevant. We verified numerically that the spin projection along the effective magnetic field $\mathbf{B}^{inst}$ given by Eq. (10), is well conserved while the spin projection along the real magnetic field $\mathbf{B}$ evidences time dependent oscillations, as already stated by Ref. [10].

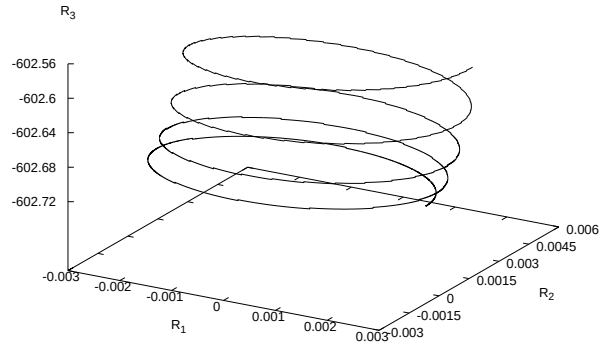

FIG. 2: Plot of a 3−D trajectory originated by initial conditions close to those corresponding to the micromotion. The numbers on the axes express the coordinates in μm. This trajectory corresponds to 5 times the $2\pi/\omega_T$ period. It is not closed, while a stable micromotion orbit corresponds to a closed motion. The number on the axes express the coordinates in μm.

We have explored a different region of parameter values, where we expect the adiabatic approximation to break down. While the adiabaticity is certainly not fulfilled if $\omega_z, \omega_r \sim \omega_L$, a further source of failure for this approximation rests in the intensity of the geometric magnetic fields of Eqs. (49) being of the same order of magnitude of the applied real ones. This occurs, for example, at bias field intensities of the order of $B_0 = 2.\ 10^{-7}$T. Notice that for this weak rotating RF field, the trap oscillation frequencies of Eq. (19) are large enough to sustain the atoms against gravity. However the radius ρ of the circle of death of Eq. (11) becomes comparable to the radius r of the micromotion orbit. Fig. 3 (a),(b) and (c) show the components of $\mathcal{B}$ as a function of time obtained with initial conditions very close to those of a micromotion orbit. For this set of parameters it is interesting to make a comparison between the atom dynamics generated by the classical equation of motion and the effective improved equations of motion. The latter give rise to a stable motion, shown in Fig. 3(d) traced by integrating the effective equations (46) and (48). Under the same initial conditions the classical equations of motion generate an unstable trajectory with the atoms conserving initially a constant height $z = 0.73\mu$m, and then after several milliseconds escaping from the trap. The more stable character of the effective equations solution in respect to the classical ones is made evident by comparing the spin projection along $\mathbf{B}^{inst}$ in both cases. By numerically integrating the effective equations (46) and (48), we found oscillations of $\mathcal{S}\cdot\mathbf{B}^{inst}/|\mathcal{S}||\mathbf{B}^{inst}|$ near the sta-

ble value 1. On the contrary, by integrating the classical equations (7), we found spin flip that causes the condensate escape from the trap.

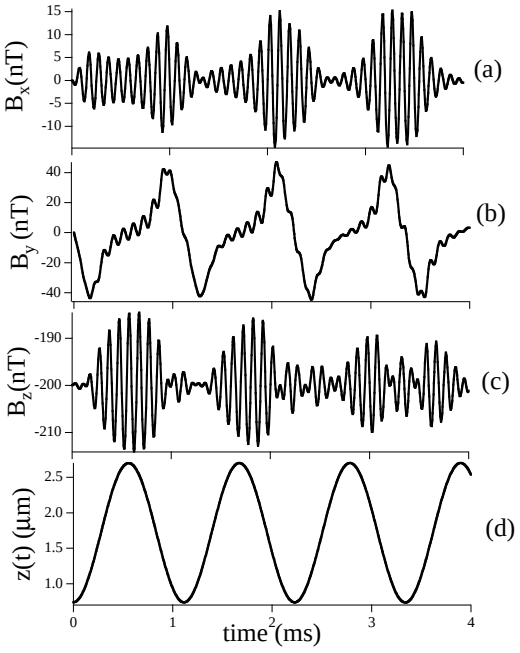

FIG. 3: In (a), (b) and (c) plots of the $\mathcal{B}_x$, $\mathcal{B}_y$, and $\mathcal{B}_z$ geometric fields, in units of $1.\times 10^{-9}$T, as a function of time in ms for atomic motion within a TOP trap with a RF bias field of 200 nT. In(d) the $z-$position, in μm, of the atomic center of mass traced by integrating the effective equations (46). Instead the integration of the classical equations of motion (7) displays an unstable trajectory.

The important role played by the terms originated by the non adiabatic approximation appears very clearly when we compared the atomic equilibrium within the TOP $z_{\rm eq}$ as derived by the classical solution to that predicted by the effective Eqs. (46) and (48). That comparison is shown in Fig. 4 for a fixed quadrupole field $b = 0.18$T/m and a RF rotating field B_0 between $1.\times 10^{-4}$T and $2.\times 10^{-7}$T. At large values of B_0 the values $z_{\rm eq}$ predicted by the classical solution and the improved one coincide. Instead the two values are different at small values of B_0 because the two solutions predict different equilibrium positions. Finally, for $B_0 < 5.\times 10^{-7}$T, classically the atoms are not suspended against gravity, while the effective equations predict a stable equilibrium position.

VII. CONCLUSIONS

In this paper we have analyzed the motion of neutral atoms within TOP magnetic traps. We have considered the approximate classical equations of motion describing such system and revisited the fast degrees of freedom motion at the forcing frequency ω_T known as

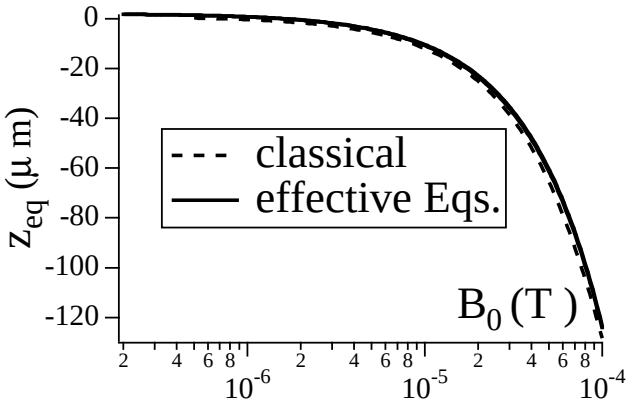

FIG. 4: Comparison between the equilibrium positions $z_{\rm eq}$ of rubidium atoms within the TOP trap versus the $B_{\rm o}$ RF field as predicted by the classical solution and by the effective equations (46) and (48) at a given value of the quadrupole field gradient $b = 0.18$T/m. For $B_0 < 5.\times 10^{-7}$T, the classical model does not leads to a stable orbit.

atomic micromotion. In such a motion non-adiabatic effects and geometric fields are absent. Within the scenario of adiabatic approximation, we have analyzed the atomic quantum motion by taking into account the lowest frequencies terms embodied into the time-dependent potential. Within this approximation, the center-of-mass motion resulting harmonic, we have calculated the harmonic trapping frequences and recovered the quantum counterpart of the classical micromotion. Addressing the problem within a pure quantum context, as a consequence of the presence of inhomogeneous magnetic fields geometric magnetic fields appear quite naturally. These geometric fields are responsible for a misalignment of the atomic spin with respect to the local magnetic field and then for non-adiabatic effects. Within this framework, we have derived an effective classical dynamics in which these geometric fields are explicitly embodied. The atomic motion results by the coupling of a quantum harmonic motion, governing the center of mass, and an effective nonlinear spin dynamics driven by both the local magnetic field and the geometric ones.

The numerical simulations performed for the parameters of standard experimental set-ups have shown that the adiabatic approximation is well suited. On the other hand, by reducing the intensity of the bias field, non-adiabatic effects show up, because the geometric field becomes more relevant and cause misalignment of the spins around $\mathbf{B}^{inst}$.

Another relevant facet concerns the sensitivity to the initial condition of the trap equations. The projection of the atomic magnetic moment on the local field $\mathbf{B}^{inst}$ is a conserved quantity, an adiabatic integral. The initial condition of $\mathbf{S}\cdot\mathbf{B}^{inst}$ chosen for a given simulation identifies a given dynamical evolution, its value remaining conserved during atomic motion. On the other hand, the equilibrium height is determined by the value of this

quantity [see Eq. (25)], so that the projection of the atomic magnetic moment on the local field determines the cloud equilibrium height. Now, it is a fact that, for a given geometry of magnetic fields within a trap, such a height results to be independent on the initial preparation condition. Thus, since the dynamical equations do not select by itself any special value of this quantity, one could argue, in order to explain some experimental features of the BEC clouds [11, 12], that a possible modification of the actual spin projection on $\mathbf{B}^{inst}$ might by involved in some steps of the preparation of the relative Bose-Einstein condensate. Further attention should also be devoted to the non-linear interaction within the condensate.

VIII. ACKNOWLEDGMENTS

This work has progressed through the constant collaboration of several members of the BEC group in Pisa, M. Anderlini, D. Ciampini. R. Mannella, O. Morsch, J.H. Müller, and through useful discussions with M. Mintchev.

APPENDIX A: ABOUT THE SU(2) ALGEBRA

The su(2) algebra is defined starting from the angular momentum generators s_x, s_y, s_z and their commutation relations. Using the standard definitions for the raising and lowering operators, we derive the following relations for the derivatives of the operator $M(\phi,\theta)$ defined in Eq. (31)

$$\begin{aligned}
M^\dagger(\varphi,\vartheta)\partial_\varphi M(\varphi,\vartheta) =& -\frac{i}{\hbar}(s_z\cos\vartheta - s_x\sin\vartheta)\,,\\
M^\dagger(\varphi,\vartheta)\partial_\vartheta M(\varphi,\vartheta) =& -\frac{i}{\hbar}s_y\,,\\
M^\dagger(\varphi,\vartheta)\partial^2_{\varphi\varphi} M(\varphi,\vartheta) =& -\frac{1}{\hbar^2}(s_z\cos\vartheta - s_x\sin\vartheta)^2\,,\\
M^\dagger(\varphi,\vartheta)\partial^2_{\vartheta\vartheta} M(\varphi,\vartheta) =& -\frac{1}{\hbar^2}s_y^2\,,\\
M^\dagger(\varphi,\vartheta)\partial^2_{\varphi\vartheta} M(\varphi,\vartheta) =& -\frac{1}{\hbar^2}(s_z\cos\vartheta - s_x\sin\vartheta)s_y\,,\\
M^\dagger(\varphi,\vartheta)s_x M(\varphi,\vartheta) =& s_x\cos\vartheta\cos\varphi - s_y\sin\varphi +\\
& s_z\sin\vartheta\cos\varphi\,,\\
M^\dagger(\varphi,\vartheta)s_y M(\varphi,\vartheta) =& s_x\cos\vartheta\sin\varphi + s_y\cos\varphi +\\
& s_z\sin\vartheta\sin\varphi\,.
\end{aligned} \tag{A1}$$

APPENDIX B: GEOMETRIC TERMS

For a cylindric TOP trap with magnetic field as defined in (5), the geometric fields result

$$\begin{aligned}
\nabla\vartheta =& \frac{b}{(B^{\rm R})^2\sqrt{(B^{\rm R}_x)^2+(B^{\rm R}_y)^2}}\begin{bmatrix} B^{\rm R}_z\, b(x+\rho\cos\omega_T t)\\ B^{\rm R}_z\, b(y+\rho\sin\omega_T t)\\ 2[(B^{\rm R}_x)^2+(B^{\rm R}_y)^2]\end{bmatrix}\,,\\
\nabla\varphi =& \frac{b^2}{(B^{\rm R}_x)^2+(B^{\rm R}_y)^2}\begin{bmatrix} -y-\rho\sin\omega_T t\\ x+\rho\cos\omega_T t\\ 0\end{bmatrix}\,,\\
\partial_t\vartheta =& \frac{\omega_T b^2 B^{\rm R}_z}{(B^{\rm R})^2\sqrt{(B^{\rm R}_x)^2+(B^{\rm R}_y)^2}}\,\rho\,(y\cos\omega_T t - x\sin\omega_T t)\,,\\
\partial_t\varphi =& \omega_T\left(\frac{b\rho B^{\rm R}_x}{(B^{\rm R}_x)^2+(B^{\rm R}_y)^2}-1\right)\,,\\
\Delta\vartheta =& \frac{B^{\rm R}_z}{\sqrt{(B^{\rm R}_x)^2+(B^{\rm R}_y)^2}}\left(1+6\frac{(B^{\rm R}_x)^2+(B^{\rm R}_y)^2}{(B^{\rm R})^2}\right)\,,\\
&\nabla\varphi\nabla\vartheta = 0\,,\quad \Delta\varphi = 0\,.
\end{aligned} \tag{B1}$$

APPENDIX C: TDVP APPROACH

In our contest the TDVP method structures the dynamical quantum-state describing the atomic motion, in terms of a trial state written, as in Eq. (37), as the product of a time-dependent phase factor $e^{-iS(t)/\hbar}$ times a spatial- and time-dependent scalar wave function $\Psi(\mathbf{x},t)$ times a time-dependent spinor $|j,\tau(t)\rangle$. The time-dependent trial state $\psi(\mathbf{x},t)$ is to be found in a self-consisting way. By imposing the weaker form of the Schrödinger equation

$$\int d\mathbf{x}\,\psi^\dagger(\mathbf{x},t)\left[i\hbar\partial_t - H^{\rm R}\right]\psi(\mathbf{x},t) = 0\,, \tag{C1}$$

we get the effective action $S(t)$

$$\begin{aligned}
S(t) =& \int_0^t dt\\
&\int d\mathbf{x}\,\langle j,\tau(t)|\Psi^\dagger(\mathbf{x},t)\left[i\hbar\partial_t - H^{\rm R}\right]\Psi(\mathbf{x},t)|j,\tau(t)\rangle\,.
\end{aligned}$$

By splitting the Hamiltonian as $H^{\rm R} = H^\sigma_{ad} + \Delta H^\sigma$, where H^σ_{ad} has been introduced in (14), we get

$$\begin{aligned}
S(t) =& \int_0^t dt\,\int d\mathbf{x}\,\Psi^\dagger(\mathbf{x},t)\left[i\hbar\partial_t - H^\sigma_{ad}\right]\Psi(\mathbf{x},t) +\\
&\int_0^t dt\,\int d\mathbf{x}\,\langle j,\tau(t)|\left[i\hbar|\Psi(\mathbf{x},t)|^2\partial_t -\right.\\
&\left.\Psi^\dagger(\mathbf{x},t)\Delta H^\sigma\Psi(\mathbf{x},t)\right]|j,\tau(t)\rangle\,.
\end{aligned} \tag{C2}$$

By expanding the Hamiltonian H^σ_{ad} in a power series of the displacement coordinates $(x,y,\zeta = z-h)$, we get

the harmonic Hamiltonian with the time-dependent potential of Eq. (16). Thus, by introducing the structure $\Psi(\mathbf{x},t)$ of Eq. (20) for the atomic wave function we find the Schrödinger Eq. (22). After taking the time average of the latter equation on a short time $2\pi/\omega_T$, we get the harmonic problem (23) of which the general solution $\Phi(\mathbf{x},t)$ is known. Thus, the first term in the r.h.s. in Eq. (C2) vanishes, and we obtain

$$S(t) = \int_0^t dt\, \langle j,\tau(t)| \left[i\hbar\partial_t - \langle \Delta H^\sigma_{(2)} \rangle \right] |j,\tau(t)\rangle \,,$$

where $\langle \Delta H^\sigma_{(2)} \rangle = \int d\mathbf{x}\, [\Psi^\dagger(\mathbf{x},t) \Delta H^\sigma_{(2)} \Psi(\mathbf{x},t)]$ and $\Delta H^\sigma_{(2)}$ is obtained by expanding ΔH^σ in a power series in $\mathbf{x}$ and $\mathbf{p}$ up to the second order. Explicitly we have

$$\langle \Delta H^\sigma_{(2)} \rangle = \sum_i \langle h^i_{(2)} \rangle s_i + \sum_{jk} \langle g^{jk}_{(2)} \rangle s_j s_k - \langle \sigma \mu B^{\rm R}_{(2)} \rangle \,,$$

with the obvious meaning of index (2).

The Hamiltonian $\langle \Delta H^\sigma_{(2)} \rangle$ is built of su(2) algebra generators acting on the time-dependent spin vector $|j,\tau(t)\rangle$. We choose for $|j,\tau(t)\rangle$ the components of the su(2) atomic coherent state $|\tau(t)\rangle$ of j representation. As a support for this choice let us remember that, if the Hamiltonian $\langle \Delta H^\sigma_{(2)} \rangle$ was a closed dynamical algebra, *i.e.* a linear combination of the su(2) generators, the solutions of the Schrödinger equation given by these coherent states would be exact [27]. The equation of motion for the label $\tau(t)$ (and its complex conjugate), that involves the dynamical evolution of the state $\psi(\mathbf{x},t)$, is obtained by stationarizing the effective action $S(t)$

$$\delta S = \delta \left(\int_0^t dt \left\{ i\hbar\, \langle j,\tau(t)| \left[\dot\tau \frac{d}{d\tau} + \dot{\bar\tau} \frac{d}{d\bar\tau} \right] |j,\tau(t)\rangle - \langle j,\tau(t)|\langle \Delta H^\sigma_{(2)} \rangle |j,\tau(t)\rangle \right\} \right) = 0 \,. \tag{C3}$$

After boring algebra we get the equations of motion

$$\frac{d\tau}{dt} = \frac{(1+|\tau|^2)^2}{2i\hbar j}\, \partial_{\bar\tau} \mathcal{H}(\tau,\bar\tau) \,,$$

where $\mathcal{H}(\tau,\bar\tau) = \langle \tau|\langle \Delta H^\sigma_{(2)} \rangle|\tau\rangle$ and $\bar\tau$ is the complex conjugate of τ. These tricky equations can be cast in more familiar form by writing them in terms of the classical spin components $\mathcal{S}_{\rm x}, \mathcal{S}_{\rm y}, \mathcal{S}_{\rm z}$ introduced in the text. The dynamics of these spin components, apart terms irrelevant for the equations of motion, is generated by the following Hamiltonian:

$$\mathcal{H}(\mathcal{S}_{\rm x},\mathcal{S}_{\rm y},\mathcal{S}_{\rm z}) = \sum_i \langle h^i_{(2)} \rangle \mathcal{S}_i + (1-\frac{1}{2j}) \sum_i \langle g^{ii}_{(2)} \rangle \mathcal{S}_i^2 + 2(1-\frac{1}{2j}) \langle g^{xz}_{(2)} \rangle \mathcal{S}_{\rm x} \mathcal{S}_{\rm z} \,, \tag{C4}$$

where the time-dependent coefficients are derived by the center of mass wave function $\Psi(\mathbf{x},t)$ as

$$\langle h^i_{(2)} \rangle = \int d\mathbf{x}\, [\Psi^\dagger(\mathbf{x},t) h^i_{(2)} \Psi(\mathbf{x},t)] \quad \text{for } i = x,y,z \,,$$
$$\langle g^{ij}_{(2)} \rangle = \int d\mathbf{x}\, [\Psi^\dagger(\mathbf{x},t) g^{ij}_{(2)} \Psi(\mathbf{x},t)] \quad \text{for } i,j = x,y,z \,, \tag{C5}$$

the operators h^i and g^{ij} have been given in (36). Therefore we obtain a canonical system for the classical spin components whose dynamics is generated by the effective Hamiltonian $\mathcal{H}$, endowed with the Poisson brackets $\{\mathcal{S}_{\rm x},\mathcal{S}_{\rm y}\} = \mathcal{S}_{\rm z}$ and cyclic permutations.

[1] For an introduction see a supplement in Sakurai *Modern Quantum Mechanics* (Addison Wesley, Boston, 1994). For a review see A. Shapere and F. Wilczek, *Geometric phases in Physics* (World Scientific, Singapore, 1989). For a list of experiments on Berry's phase see J. Anandan, J. Christiam, and K. Wakelik, Am. J. Phys. **65**, 180 (1997).

[2] An early study of the non-adiabatic processes for the atomic motion within an inhomogeneous magnetic field was made by E. Majorana, Nuovo Cimento **9** 44 (1932).

[3] Y. Aharonov and A. Stern, Phys. Rev. Lett. **69**, 3593 (1992).

[4] An additional velocity-dependent potential is derived in R.G. Littlejohn and S. Weigert, Phys. Rev. A **48**, 924 (1993).

[5] C.-P. Sun, M.-L. Ge, and Q. Xiao, Commun. Theor. Phys. **13** 63 (1990); C.-P. Sun, M.-L. Ge, Phys. Rev. D **41**, 1349 (1990).

[6] T.-L. Ho and V.B. Shenoy, Phys. Rev. Lett. **77**, 2595 (1996).

[7] C.V. Sukumar and D.M. Brink, Phys. Rev. A **56**, 2451 (1997).

[8] E.A. Hinds and C. Eberlein, Phys. Rev. A **61**, 033614 (2000).

[9] R.M. Potvliege and V. Zehnlé, Phys. Rev. A **63**, 025601 (2001).

[10] J. Schmiedmayer and A. Scrinzi, Quantum Semiclass. Opt. **8**, 693 (1996); J.R. Anglin and J. Schmiedmayer, arXiv:physics/0211062.

[11] J.H. Müller, O. Morsch, D. Ciampini, M. Anderlini, R. Mannella, and E. Arimondo, Phys. Rev. Lett. **85**, 4454 (2000).

[12] J.H. Müller, O. Morsch, D. Ciampini, M. Anderlini, R. Mannella and E. Arimondo, C. R. Acad. Sci. Paris, **t.2 IV**, 649 (2001).

[13] W. Petrich, M.H. Anderson, J.R. Ensher, and E.A. Cornell, Phys. Rev. Lett. **74**, 3352 (1995).

[14] M.H. Anderson, J.R. Ensher, M.R. Matthews, C.E. Wie-

man, and E.A. Cornell, Science **269**, 198 (1995).
[15] E.W. Hagley , L. Deng, M. Kozuma, J. Wen, K. Helmerson, S.L. Rolston, and W.D. Phillips, Science **283**, 1706 (1999).
[16] D.J. Han, R.H. Wynar, Ph. Courteille, and D.J. Heinzen, Phys. Rev. A **57**, R4114 (1998).
[17] B.P. Anderson and M.A. Kasevich, Phys. Rev. A **59**, R938 (1999).
[18] J. L. Martin, C.R. McKenzie, N.R. Thomas, J.C. Sharpe, D.M. Warrington, P.J. Manson, W.J. Sandle and A.C. Wilson, J. Phys. B: Atom. Mol. Opt. Phys. **32**, 3065 (1999).
[19] J. Arlt, O. Maragó, E. Hodby, S.A. Hopkins, G. Hechenblaikner, S. Webster, and C.J. Foot, J. Phys. B: Atom. Mol. Opt. Phys. **32**, 5861 (1999).
[20] S. Gov and S. Shtrikman, J. Appl. Phys. **86**, 2250 (1999).
[21] The different experimental configurations are characterized by the components of the quadrupole gradients along the orthogonal axes appearing in Eq. (3) and by the plane containing the rotating magnetic field of Eq. (4). The geometry of the Pisa experiment with a triaxial TOP trap corresponds to $-b_x = -b_y = b_z/2 = b$ and the B_0 field rotating in the horizontal plane[22].
[22] J.H. Müller, D. Ciampini, O. Morsch, G. Smirne, M. Fazzi, P. Verkerk, F. Fuso, and E. Arimondo, J. Phys. B: Atom. Mol. Opt. Phys. **33**, 4095 (2000).
[23] V. G. Minogin, J. A. Richmond, and G. I. Opat, Phys. Rev. A **58**, 3138 (1998).
[24] D.S. Hall, J.R. Ensher, D.S. Jin, M.R. Matthews, C.E. Wieman, and E.A. Cornell, Proc. SPIE Int. Soc. Opt. Eng. **3270**, 98 (1998).
[25] M. V. Berry, Proc. R. Soc. London A **452**, 1207-1220 (1996).
[26] R. J. Cook, D. G. Shankland, and A. L. Wells, Phys. Rev. A, **31**, 564 (1985).
[27] W. M. Zhang, D. H. Feng and R. Gilmore, Rev. Mod. Phys. **62**, 867 (1990); T. Fukui and Y. Tsue, Prog. Theor. Phys. **87**, 627 (1992); A. Montorsi and V. Penna, Phys. Rev. B, **55**, 8226 (1997).
[28] L. Mandel and E. Wolf, *Optical Coherence and Quantum Optics*, (Cambridge University, Cambridge, 1995).
[29] Since the center of mass motion is described by a 3D harmonic oscillator Hamiltonian, the center of mass wavefunction is given at all times by a Glauber coherent state $|\alpha\rangle$ representing the minimum indetermination state[28]. It is easy matter to verify that $\langle\alpha|(xp + px)/2|\alpha\rangle = \langle\alpha|x|\alpha\rangle\langle\alpha|p|\alpha\rangle$. Therefore the factorization applies to those states.